

# Antibody-mediated delivery of T-cell epitopes to antigen-presenting cells induce strong CD4 and CD8 T-cell responses



Lene S. Høydahl<sup>a,b,\*</sup>, Terje Frigstad<sup>a,b,2</sup>, Ingunn B. Rasmussen<sup>a,b</sup>, Inger Øynebråten<sup>a,1</sup>, Karoline W. Schjetne<sup>a,3</sup>, Jan Terje Andersen<sup>a,b,c</sup>, Terje E. Michaelsen<sup>d,e</sup>, Elin Lunde<sup>b</sup>, Bjarne Bogen<sup>a</sup>, Inger Sandlie<sup>a,b</sup>

<sup>a</sup> Centre for Immune Regulation and Department of Immunology, University of Oslo and Oslo University Hospital, N-0372 Oslo, Norway

<sup>b</sup> Centre for Immune Regulation and Department of Biosciences, University of Oslo, N-0316 Oslo Norway

<sup>c</sup> Department of Pharmacology, Institute of Clinical Medicine, University of Oslo and Oslo University Hospital, N-0318 Oslo, Norway

<sup>d</sup> Department of Infection Immunology, Norwegian Institute of Public Health, N-0403 Oslo, Norway

<sup>e</sup> School of Pharmacy, University of Oslo, N-0316 Oslo, Norway

## ARTICLE INFO

### Article history:

Received 1 September 2020

Received in revised form 12 January 2021

Accepted 6 February 2021

Available online 19 February 2021

### Keywords:

Antibody engineering

Antigen presentation

Subunit vaccine

Cross-presentation

APC targeting

T-cell activation

## ABSTRACT

Targeted delivery of antigen to antigen-presenting cells (APCs) enhances antigen presentation and thus, is a potent strategy for making more efficacious vaccines. This can be achieved by use of antibodies with specificity for endocytic surface molecules expressed on the APC. We aimed to compare two different antibody-antigen fusion modes in their ability to induce T-cell responses; first, exchange of immunoglobulin (Ig) constant domain loops with a T-cell epitope (Troybody), and second, fusion of T-cell epitope or whole antigen to the antibody C-terminus. Although both strategies are well-established, they have not previously been compared using the same system. We found that both antibody-antigen fusion modes led to presentation of the T-cell epitope. The strength of the T-cell responses varied, however, with the most efficient Troybody inducing CD4 T-cell proliferation and cytokine secretion at 10–100-fold lower concentration than the antibodies carrying antigen fused to the C-terminus, both *in vitro* and after intravenous injection in mice. Furthermore, we exchanged this loop with an MHCII-restricted T-cell epitope, and the resulting antibody enabled efficient cross-presentation to CD8 T cells *in vivo*. Targeting of antigen to APCs by use of such antibody-antigen fusions is thus an attractive vaccination strategy for increased activation of both CD4 and CD8 peptide-specific T cells.

© 2021 The Authors. Published by Elsevier Ltd. This is an open access article under the CC BY license (<http://creativecommons.org/licenses/by/4.0/>).

## 1. Introduction

Induction of robust T-cell responses is of high relevance for vaccine efficacy. Such immune activation requires interaction between antigen-presenting cells (APCs) that present antigenic peptides on MHC molecules and T cells that recognize the peptide

MHC complexes by specific T-cell receptors [1]. All nucleated cells express MHCII molecules and present endogenously derived peptides to CD8 cytotoxic T cells. In contrast, steady-state expression of MHCII is restricted to professional APCs, which includes B cells, dendritic cells (DCs) and macrophages (Mfs). These cells are responsible for presentation of exogenously derived peptides on MHCII to CD4 T cells. There is however, plasticity in the antigen presentation pathways, allowing endocytosed antigens to be presented on MHCI by cross-presentation [1–3].

Subunit vaccines typically consist of pathogen-derived proteins or peptides [4]. Proteins that contain both CD4 and CD8 T-cell epitopes as well as B-cell epitopes may elicit broad immune responses. However, some protein antigens are not readily soluble or may have toxic effects. Thus, an alternative is use of vaccines that consist of antigenic T-cell epitopes only, and such vaccines may be particularly useful whenever T cells play the main role in immune protection [5].

**Abbreviations:** APCs, antigen presenting cells; Ig, immunoglobulin; DCs, dendritic cells; Mfs, macrophages; C-t, C-terminal; LLO, Listeriolysin-O; wt, wild-type; TCC, T-cell clone; h, human.

\* Corresponding author at: Centre for Immune Regulation and Department of Immunology, University of Oslo and Oslo University Hospital, N-0372 Oslo, Norway.

E-mail address: [l.s.hoydahl@medisin.uio.no](mailto:l.s.hoydahl@medisin.uio.no) (L.S. Høydahl).

<sup>1</sup> Present address: Department of Pathology, Oslo University Hospital and University of Oslo, N-0372 Oslo, Norway.

<sup>2</sup> Present address: Nextera AS, N-0349 Oslo, Norway.

<sup>3</sup> Present address: Vaccibody AS, N-0349 Oslo, Norway.

<https://doi.org/10.1016/j.vaccine.2021.02.012>

0264-410X/© 2021 The Authors. Published by Elsevier Ltd.

This is an open access article under the CC BY license (<http://creativecommons.org/licenses/by/4.0/>).

Furthermore, the immune response may be strengthened by increasing the amount of antigen that is presented by the APCs. This can be done by specifically targeting antigen to APCs by use of antibodies with specificity for APC surface molecules [6–9]. Antibodies are suitable carriers as they may bind their target with high specificity and affinity. A widely used strategy is to chemically conjugate whole antigen to the antibody [8]. An alternative strategy is to genetically integrate the antigenic epitope as a part of the antibody, for instance by replacing loops in immunoglobulin (Ig) domains with the epitope sequence, in so called Troybodies [6,10–15]. We have previously explored the latter strategy by sequential exchange of all six loops connecting  $\beta$ -strands (L1–L6) of the three Ig constant domains (CH1, CH2, CH3) with T-cell epitopes [11]. Considering both antibody secretion level from producing cells and T-cell activation efficiency, we found that a total of eight loops may carry T-cell epitopes to APCs, namely, all in CH2 in addition to L6 in CH1 and CH3. Comparison of L4CH2 with L6CH1 Troybodies after injection of antibodies in BALB/c mice, revealed that L4CH2 was by far the most efficient and induced specific T-cell activation at concentrations at least 100-fold lower than L6CH1 [11].

Here, we extend the study by directly comparing the potency of such Troybodies carrying antigenic peptide integrated as Ig loops with antibodies with antigen or peptide genetically fused to the Ig C-terminal (C-t) end. We included L6CH1 and L4CH2 in the study, as well as L4CH1, as these Troybodies induce of T-cell responses ranging from weak to potent activation. The model tumor antigen used is derived from the M315 IgA myeloma protein, secreted by the MOPC315 myeloma cell line [16]. M315 IgA contains an I-E<sup>d</sup>-restricted CD4 T-cell epitope within a fragment spanning amino acid (aa) 89–105 of the  $\lambda 2$  light chain,  $\lambda 2^{315}$  (herein denoted  $\lambda$ ) [17]. In addition to genetically fusing the  $\lambda$  T-cell epitope to the C-t end of the Ig heavy chain, we also fused the whole scFv derived from M315 to the Ig C-terminus. In brief, we found that the *in vitro* T-cell response induced by the  $\lambda$  L4CH2 antibody was 10–100-fold more efficient than  $\lambda$  L4CH1,  $\lambda$  L6CH1 and both the C-t antigen fusions. Moreover, the  $\lambda$  L4CH2 antibody was also the most potent after *in vivo* targeting. Furthermore, we studied whether this particular loop would be suitable for insertion of a MHCI-restricted epitope for cross-presentation and activation of CD8 T cells by inserting an immunodominant CD8 T-cell epitope (aa 91–99 of Listeriolysin-O (LLO), the epitope herein denoted LLO) from a *Listeria monocytogenes* [18]. Indeed, an antibody carrying LLO in L4CH2 targeted APCs and induced cross-presentation to CD8 T cells *in vivo*. This demonstrates that a Troybody may carry both MHCI and MHCII epitopes for induction of strong T-cell responses, which encourages further investigation of such antibody-antigen fusions as subunit vaccines.

## 2. Materials and methods

### 2.1. Construction of recombinant antibodies

Recombinant antibodies were constructed and produced from expression vectors pLNOH2 oriP and pLNOk oriP encoding human (h) IgG3 C $\gamma$ 3 heavy chain and hC $\kappa$  light chain, respectively [19]. The recombinant Ig heavy chains were placed downstream of V regions encoding specificity of either mouse IgD (clone Ig(5a)7.2) [6], mouse CD40 (clone FGK45) [15], or the hapten 4-hydroxy-3-iodo-5-nitrophenylacetic acid (NIP) [20]. The IgD-specific antibodies containing the  $\lambda$  T-cell epitope (aa 89–105 of  $\lambda 2^{315}$  (FAALWFRNHFVFGGGTK)) exchanged with the native aa of loop 4 of CH1 (L4CH1 (DE loop), aa QSSGL), loop 6 of CH1 (L6CH1 (FG loop), aa KPSN) and loop 4 of CH2 (L4CH2), aa YNST) of hIgG3 have been described previously [10,11]. Loops were identified based on IMGT Ig annotations and the cysteine originally present in position 90 of the  $\lambda$  epitope was changed to an alanine. The expression vector pLNOH2 hIgG3 anti-NIP  $\lambda$  L4CH2 oriP was generated by subcloning the C $\gamma$ 3 genes on the restriction enzymes BsiWI and BamHI into pLNOH2 anti-NIP oriP. Fusion of 89–105 of  $\lambda 2^{315}$  to the C-terminal of the hIgG3 heavy chain was done by PCR-SOEing [21]. Briefly, two separate PCRs were set up using the primer pairs lambda\_fw/BamHI\_rv or lambda\_rv/BmgBI\_fw (Table 1). PCR was performed using Phusion DNA polymerase according to protocol. A new PCR was set up to combine the two first PCR product together using the purified, first PCR products as templates and the primers BmgBI\_fw and BamHI\_rv. The final PCR product was cloned into pLNOH2 hIgG3 anti-IgD oriP using the restriction sites BmgBI and BamHI. During construct generation a double BmgBI site was created, which was subsequently removed by cloning into a clean vector backbone. To fuse the scFv based on M315 to the hIgG3 heavy chain C-terminus, a BspEI restriction enzyme site was first created at the end of the CH3 domain of pLNOH2 hIgG3 anti-IgD oriP by QuikChange site-specific mutagenesis (Agilent technologies) using Pfu Turbo DNA polymerase (Stratagene, #600252) and the primers Q\_BspEI\_CH3\_fw and Q\_BspEI\_CH3\_rc (Table 1) according to the protocol. The M315 scFv had previously been assembled in a different vector and was PCR amplified using the primers M315\_scFv\_BspEI\_fw and M315\_scFv\_BspEI\_rv (Table 1), and cloned into the BspEI site following restriction enzyme digested. Of note, the forward primer included the sequence encoding a GGGSGGG to provide a spacer between the Ig heavy chain and the scFv. Expression vectors encoding the LLO peptide (GYKDGNEYI) in L4CH2 were generated as follows; pLNOH2 hIgG3 anti-NIP oriP was used as template for QuikChange site-directed mutagenesis using the primer pair Q\_LLO\_L4CH2\_fw/Q\_LLO\_L4CH2\_rv (Table 1) as described above to exchange the

**Table 1**

List of primers.

Primer name	Primer Sequence
Lambda_fw	5' <b>TTCCGACGCTCTATGGTTCAGAAACCACTTCTGCTTCGGTGGTGGAAACCAAGGTGAGTGCCACAGCCGG</b> 3'
Lambda_rv	5' <b>CTTGGTTCACCACCGAACAACAAGTGTGTTCTGAACCATAGAGCTCGCAA</b> TTTACCCTGGAGACAGGG 3'
BmgBI_fw	5' <b>GTGGACGCTGAGCCACG</b> 3'
BamHI_rv	5' <b>CTAGTGGATCCTCTAGAG</b> 3'
Q_BspEI_CH3_fw	5' <b>CTGTCTCCGGATAAATGAGTGCG</b> 3'
Q_BspEI_CH3_rv	5' <b>CGCACTCATTTATCCGGAGACAG</b> 3'
M315_scFv_BspEI_fw	5' <b>GGCTCCGGATAAAGCGCGGCGGAGCGGCGCGGCGAGCTGCAGTGCAGGAG</b> 3'
M315_scFv_BspEI_rv	5' <b>GGCTCCGGACTATAGGACAGTGCACCTTGGTTC</b> 3'
Q_LLO_L4CH2_fw	5' <b>GACAAAGCCGCGGGAGGAGCAGGGTTATAAGGACGGCAACGAGTACATCTCCGTGTGGTCAGCGTCTCACCG</b> 3'
Q_LLO_L4CH2_rv	5' <b>CGGTGAGGACGCTGACCACCGGAAGATGTACTCGTTCGGCTCTTATAACCTGCTCTCCCGCGCTTTGTC</b> 3'

Sequences encoding the peptides are showed in bold and restriction enzyme sites are underlined. Primers were obtained from DNA Technology AS or Medprobe/Eurogentec.

L4CH2 sequences with the sequence encoding 91–99 of LLO. HindIII/BamHI fragments containing the C $\gamma$ 3 heavy chain was moved into a clean pLNOH2 backbone encoding specificity for NIP or mouse CD40. All DNA constructs were verified by sequencing.

## 2.2. Mice, cell lines and synthetic peptides

BALB/c mice (H-2<sup>d</sup>) were obtained from Taconic farms. The TCR transgenic BALB/c mice carrying the  $\lambda$ 2<sup>315</sup>-specific and I-E<sup>d</sup>-restricted 4B2A1 TCR have been described previously [22]. HEK293E cells were obtained from ATCC (CRL-10852). The CD4 T-cell clone (TCC) 7A10B2 recognize aa 91–101 of  $\lambda$ 2<sup>315</sup> in complex with I-E<sup>d</sup> and has been described previously [23]. 7A10B2 TCC cultures were initiated at  $2 \times 10^5$  cells/ml and cultured in the presence of  $4 \times 10^6$  cells/ml BALB/c splenocytes irradiated at 20 Gy as feeder cells. The cultures were supplemented with 1  $\mu$ g/ml synthetic (89–107) $\lambda$ 2<sup>315</sup> K100 peptide (FAALWFRNHFVKGGGTKVT) and 20 U/ml IL-2. The T-cell hybridoma expressing the 4B2A1 TCR has been described previously [11]. All cells were cultured under standard conditions in DMEM supplemented with addition of 10% heat-inactivated FCS, 2 mM L-glutamine, 50U/ml penicillin, and 50U/ml streptomycin (all from Lonza) or RPMI 1640 supplemented with 10% FCS, 0.1 mM non-essential amino acids (Invitrogen), 1 mM sodium pyruvate (Invitrogen), 50  $\mu$ M monothioglycerol (Sigma-Aldrich) and 22  $\mu$ g/ml gentamycin (Sanofi Aventis). The synthetic peptides corresponding to aa 89–107 of  $\lambda$ 2<sup>315</sup> K100 (FAALWFRNHFVKGGGTKVT), 91–99 LLO (GYKDGNEYI) and a hemagglutinin peptide (IYSTVASSL) was purchased from NeoMPS, GenScript and ProImmune, respectively. The study was approved by the National Committee for Animal Experiments (Oslo, Norway), and the experiments were performed in accordance with approved guidelines and regulations.

## 2.3. Production and purification of vaccine protein

HEK293E cells were transiently transfected as previously described [24]. Recombinant antibodies used in *in vitro* T-cell assays were concentrated from supernatants by ammonium sulfate precipitation as described [11]. Antibody concentration was determined by ELISA and Western blot analysis. Recombinant antibodies used in *in vivo* targeting experiments were affinity purified from cell supernatants using protein G-conjugated Sepharose columns after filtration using 0.22  $\mu$ m filter units (Millipore, #S2GPT05RE). Bound antibodies were eluted with 0.1 M Glycine-HCl pH 2.7 and fractions were immediately neutralized by addition of 1 M Tris-HCl pH 9 (40  $\mu$ l per 1 ml fractions). Antibody-containing fractions were buffer exchanged to 1 $\times$  PBS and concentrated using Amicon Ultra Centrifugal device (Millipore, #UFC910024, 100 kDa cut-off).

## 2.4. ELISA

Levels of antibodies present in cell supernatants were determined by a hlgG3-specific ELISA. Briefly, supernatants were added to 96-well plates (Nunc) coated with 1  $\mu$ g/ml anti-hlgG3 (Zymed, #HP6047), and detected with an ALP-conjugated anti-hlgG antibody (Sigma-Aldrich, #A9544, 1:2000). An in-house generated, purified hlgG3 preparation was used as standard. To determine antibody specificity, samples were applied to plates coated with either 2  $\mu$ g/ml BSA-NIP (in-house conjugated), 4  $\mu$ g/ml mouse IgD (in-house produced) or 4  $\mu$ g/ml recombinant mouse CD40/Fc chimeric protein (R&D Systems, #1215-CD). Bound antibodies were detected with an ALP-conjugated anti-hlgG antibody. Ability of IgD-specific antibodies to bind human Fc $\gamma$ R3 and FcRn was determined by addition of titrated amount of antibody samples to plates coated with 1  $\mu$ g/ml mouse IgD. Soluble, recombinant

human GST-tagged Fc $\gamma$ RI (0.5  $\mu$ g/ml), Fc $\gamma$ RIIA-R131 (10  $\mu$ g/ml) or FcRn (0.5  $\mu$ g/ml) [24,25] were pre-incubated 15 min at room temperature with an HRP-conjugated anti-GST antibody (GE Healthcare, 1:5000) before addition to the wells. NIP-specific antibodies present in blood 9 days after immunization of mice were detected by addition of undiluted blood samples to plates were coated with 1  $\mu$ g/ml BSA-NIP (in-house conjugated). As above, an ALP-conjugated anti-hlgG antibody was used to detect bound antibodies. In common for all ELISA setups, duplicates of the samples were analyzed, 1 $\times$  PBS was used for dilution of coating reagents, 1 $\times$  PBS supplemented with 4% (w/v) non-fat skim milk powder was used to block plates prior to sample addition, 1 $\times$  PBS supplemented with 0.05% (v/v) Tween-20 was used a buffer for dilution of antibodies and for washing the plates 3 $\times$  between each layer, and each layer was incubated for 1–2 h at room temperature. Of note, in the FcRn ELISA a pH 6 buffer (6 mM Na<sub>2</sub>HPO<sub>4</sub> $\times$ 2H<sub>2</sub>O, 94 mM NaH<sub>2</sub>PO<sub>4</sub> $\times$ H<sub>2</sub>O, 150 mM NaCl, 0.05% Tween-20, pH 6.0) was used for dilution of the receptor and the detection antibody, as FcRn binds pH dependently to IgG. ALP ELISAs were developed with 1 mg/ml phosphatase substrate in diethanolamine buffer, while HRP ELISAs were developed by addition of TMB solution (Calbiochem) before absorbance reading at 405 nm or 620 nm (450 nm in the case of HCl addition), respectively.

## 2.5. Western blotting

Normalized antibody samples (1.2 ng) were preheated to 95  $^{\circ}$ C for 5 min and separated on 10% Criterion Bis-Tris XT precast gels (Bio-Rad) along with a biotinylated broad-range standard (Bio-Rad, #161-0319). Proteins were transferred onto Immobilon-P PVDF membranes (Millipore, #1PVH00010, and the blots were incubated with biotinylated anti-hlgG3 (Sigma, #B3523, 1:1000, clone HP6050) and SA-HRP (Amersham Biosciences, #RPN1231V, 1:2000) diluted in 1 $\times$  PBS containing 0.05% Tween-20 and 4% BSA. SuperSignal West Pico Chemiluminescent Substrate (Pierce, #34077) was used for detection.

## 2.6. Isolation of splenocytes

Spleens were harvested from mice into RPMI 1640 supplemented with 10% FCS, 0.1 mM non-essential amino acids (Invitrogen), 1 mM sodium pyruvate (Invitrogen), 50  $\mu$ M monothioglycerol (Sigma-Aldrich) and 22  $\mu$ g/ml gentamycin (Sanofi Aventis) on ice. Single-cell suspensions were generated by pressing the organ through a tea strainer, followed by rinsing with medium. The single-cell suspension was centrifuged at 1200 rpm, for 7 min at 4  $^{\circ}$ C and resuspended in 5 ml ACT solution. Erythrocytes were lysed by incubation on ice for 5 min. The reaction was stopped by addition of medium and the cells were washed twice by centrifugation in 10 ml cold medium.

## 2.7. *In vitro* T-cell activation assay

Irradiated (20 Gy) BALB/c splenocytes were cultured at  $5 \times 10^5$  cells/well with  $2 \times 10^4$  7A10B2 T cells/well or  $1 \times 10^5$  4B2A1 LN cells/well in flat-bottomed 96-well cell culture plates together with antibodies or synthetic (89–107) $\lambda$ 2<sup>315</sup> peptide 5-fold diluted in triplicates. Supernatant samples were removed after 96 h for cytokine analysis and the cultures were replenished with new medium and pulsed with 1  $\mu$ Ci/well 3H-thymidine (Hartman Analytic, #6032). Cells were harvested (Tomtec Harvester) onto filters after 24 h and incorporated thymidine was measured using 1450 MicroBeta TriLux scintillation counter (Wallac Perkin-Elmer). Cytokine secretion was quantified by ELISA using plates coated with 2  $\mu$ g/ml anti-mouse IFN- $\gamma$  antibody (AN18.17.24) or anti-mouse IL-2 antibody (BD Pharmingen, #554424, clone JES6-

1A12). Bound cytokines were detected using 1 µg/ml biotinylated anti-mouse IFN-γ (XMG1.2) or biotinylated anti-mouse IL-2 (BD Pharmingen, #554426, clone JES6-5H4), followed by ALP-conjugated streptavidin (GE Healthcare, #1234V1, 1:3000). Plates were developed as described above. An IFN-γ preparation and recombinant mouse IL-2 (BioLegend, #575409) were used as standards.

## 2.8. In vivo targeting

BALB/c mice were injected intravenously in the tail vein with titrated amounts of purified antibodies or PBS only as described [11]. Mice were sacrificed 90 min after the injections by cervical dislocation and the spleens were removed. Splenocytes were irradiated at 8 Gy and cultured at  $5 \times 10^5$  cells/well with responder T cells; either 7A10B2 TCCs or BW 4B2A1 hybridoma T cells (both  $2 \times 10^4$ /well). Portions of supernatant were collected after 72 h for cytokine measurements, and the cultures were replenished with new medium and pulsed with 1 µCi/well 3H-thymidine. Cells were harvested after 24 h, and incorporated thymidine was measured using TopCount NXT scintillation counter (GMI). IFN-γ and IL-2 in supernatants were detected as after *in vitro* T-cells activation assay.

## 2.9. Purification of DNA plasmids for DNA immunization and immunization

Antibody-encoding plasmid DNA for DNA immunization was purified from *E. coli* Top10F (Life Technologies, # C303003) using

EndoFree Plasmid Mega Kit (QIAGEN, #12381) essentially as described in the protocol, except that pelleted DNA was dissolved in 0.9% NaCl (B. Braun Melsungen AG, #7533). Mice were anaesthetized prior to intradermal injection of antibody-encoding plasmid DNA according to the procedure described by Roos A-K et al [26]. Briefly, anesthetized mice were shaved and sprayed with alcohol near the base of the tail, before 70 µg plasmid DNA (35 µg of each heavy and light chain encoding plasmid dissolved in 25 µl 0.9% NaCl) was injected into the dermis on each side of the back. As a negative control, mice were injected with a similar volume of NaCl (0.9%). Immediately after injection, electrodes were placed over the injection site and voltage was applied (2 pulses, 1125 V/cm, 50 µsec + 8 pulses, 275 V/cm, 10 msec) using a PA-4000S-Advanced PulseAgile Rectangular Wave Electroporation System (Cyto Pulse Sciences, Inc).

## 2.10. IFN-γ ELISPOT

LLO-specific cellular recall responses were assessed by IFN-γ ELISPOT. Spleens from mice were crushed by a steel mesh to form single-cell suspensions, and treated for 5–10 min with 140 mM NH<sub>4</sub>Cl in Tris-buffer (pH = 7.2) to lyse the erythrocytes. MultiScreenHTS-IP Filter Plates (Millipore, #MSIPS4510) were pre-treated with 40 µl 35% ethanol per well for 1 min before washing twice with 150 µl sterile PBS, which also was used in the subsequent washing steps, unless otherwise noted. Plates were then coated over-night at 4 °C with 75 µl anti-mouse IFN-γ diluted in sterile PBS (12 µg/ml, clone AN-18.17.24). After washing the plates 3 times,  $1 \times 10^6$  and  $5 \times 10^5$  splenocytes in RPMI 1640 with 10%

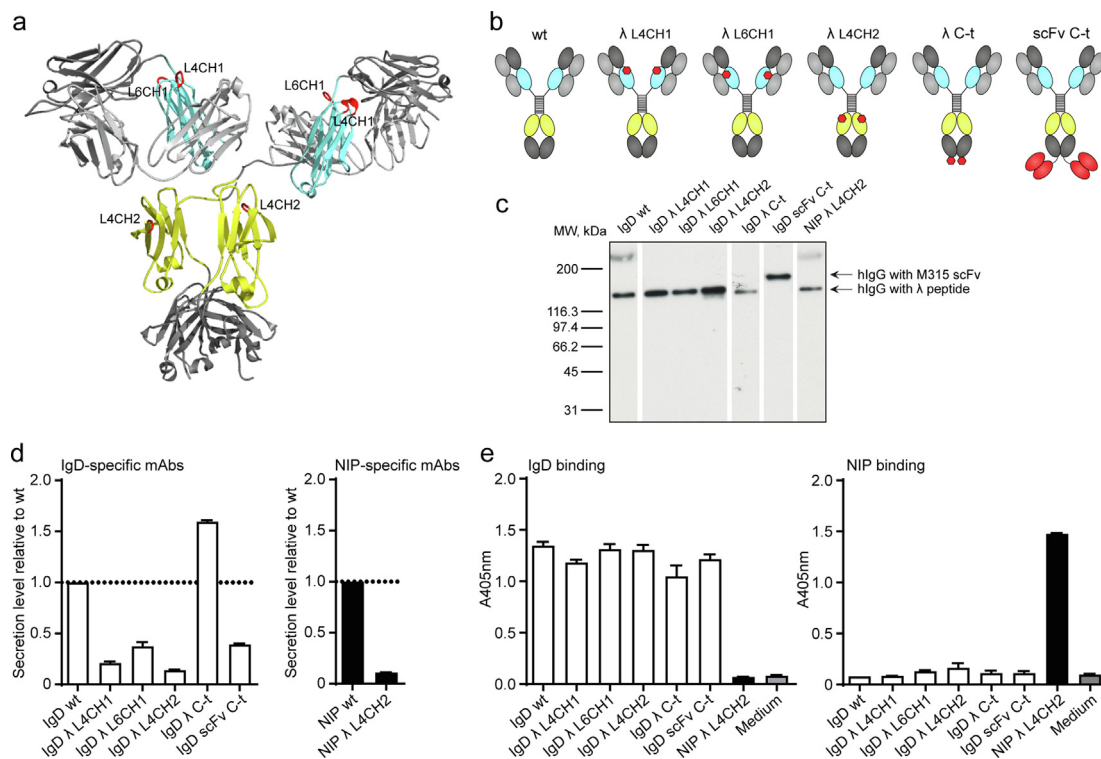


**Fig. 1.** Antibodies with loop substitutions and C-terminal fusions remain structurally and functionally intact. (a) Ribbon illustration of hlgG (PDB ID 1HZH [60]) indicating the position of the loop sequences exchanged with peptides. CH1 and CH2 domains are cyan and yellow, respectively; loop sequences exchanged with peptide are red; and IgG heavy and light chain are dark and light grey, respectively. (b) Schematic overview of the hlgG3 antibodies carrying the  $\lambda_{2315}$  epitope (herein denoted  $\lambda$ ). The  $\lambda$  epitope (amino acids 89–105) is shown as red diamond and the M315 scFv is in red. The scFv was connected through a flexible linker. (c) Representative anti-hlgG heavy chain Western blot showing antibodies concentrated from supernatants of transfected HEK293E cells ( $n = 2$ ). The gel was run under non-reducing conditions showing full-length hlgG at approx. 150 or 180 kDa depending on the presence of a  $\lambda$  epitope or scFv fusion. (d) Secretion levels of IgD- and NIP-specific antibodies from transfected HEK293E cells was determined by ELISA after harvesting supernatants over 2 weeks. Secretion levels are shown relative to wt hlgG specific for either IgD or NIP as indicated ( $n = 3$ ). (e) Normalized amounts of antibodies were analyzed for target antigen binding by ELISA. Medium from untransfected cells was used as control. Error bars indicate SEM of duplicates.

FCS and gentamicin were added per well in a total volume of 100  $\mu$ l containing LLO or HA peptide at a final concentration of 5  $\mu$ g/ml or medium alone. The plates were incubated at 37 °C with 5% CO<sub>2</sub> for approximately 26 h, before washing 3 times. Remaining, adherent cells were lysed by a 5 min incubation in dH<sub>2</sub>O, before washing twice with PBS containing 0.01% (v/v) Tween-20 and a final wash with PBS. Bound IFN- $\gamma$  was detected using a biotinylated anti-IFN- $\gamma$  antibody (clone XMG1.2, 5  $\mu$ g/ml in PBS, over-night incubation at 4 °C), followed by ALP-conjugated streptavidin (diluted 1:3000, incubated 1–2 h at room temperature, Amersham Pharmacia Biotech). Spots were developed by addition of BCIP/NBT buffer solution (Zymed, #002209) and the reaction was stopped by addition of water. Plates were air dried before the number of spots was determined electronically by Zeiss KS-EliSpot-401 instrument.

### 2.11. Statistical analyses

Immune responses among groups of mice are presented as boxes with the middle line at the mean and whiskers illustrating minimum and maximum values. P values were calculated by

two-tailed *t* test by use of GraphPad Prism version 8.0.1. P values less than 0.05 (*P* less than 0.05) were considered significant. Use of experimental duplicates or triplicates as well as representation of error bars is indicated in the individual figure legends.

## 3. Results

### 3.1. IgD-specific antibodies are expressed as functional molecules

Targeting of antigen to APCs by means of fusion to APC-specific antibodies is an efficient strategy for antigen loading of APCs and induction of T-cell responses [6–9]. We first aimed to directly compare two modes of antibody-antigen fusion with regards to T-cell activation efficiency; 1) integration into Ig constant domain loops (Troybodies), and 2) fusion to the C-t end of the Ig heavy chain. To this end, we inserted the CD4 T-cell epitope  $\lambda$  (89–105 of  $\lambda 2^{315}$ ) derived from the M315 IgA myeloma protein into hIgG by exchange of Ig constant domain loops with the T-cell epitope [16,17]. We chose L4CH1, L6CH1 and L4CH2, as all have previously been shown to induce T-cell responses [11]. In addition, we con-

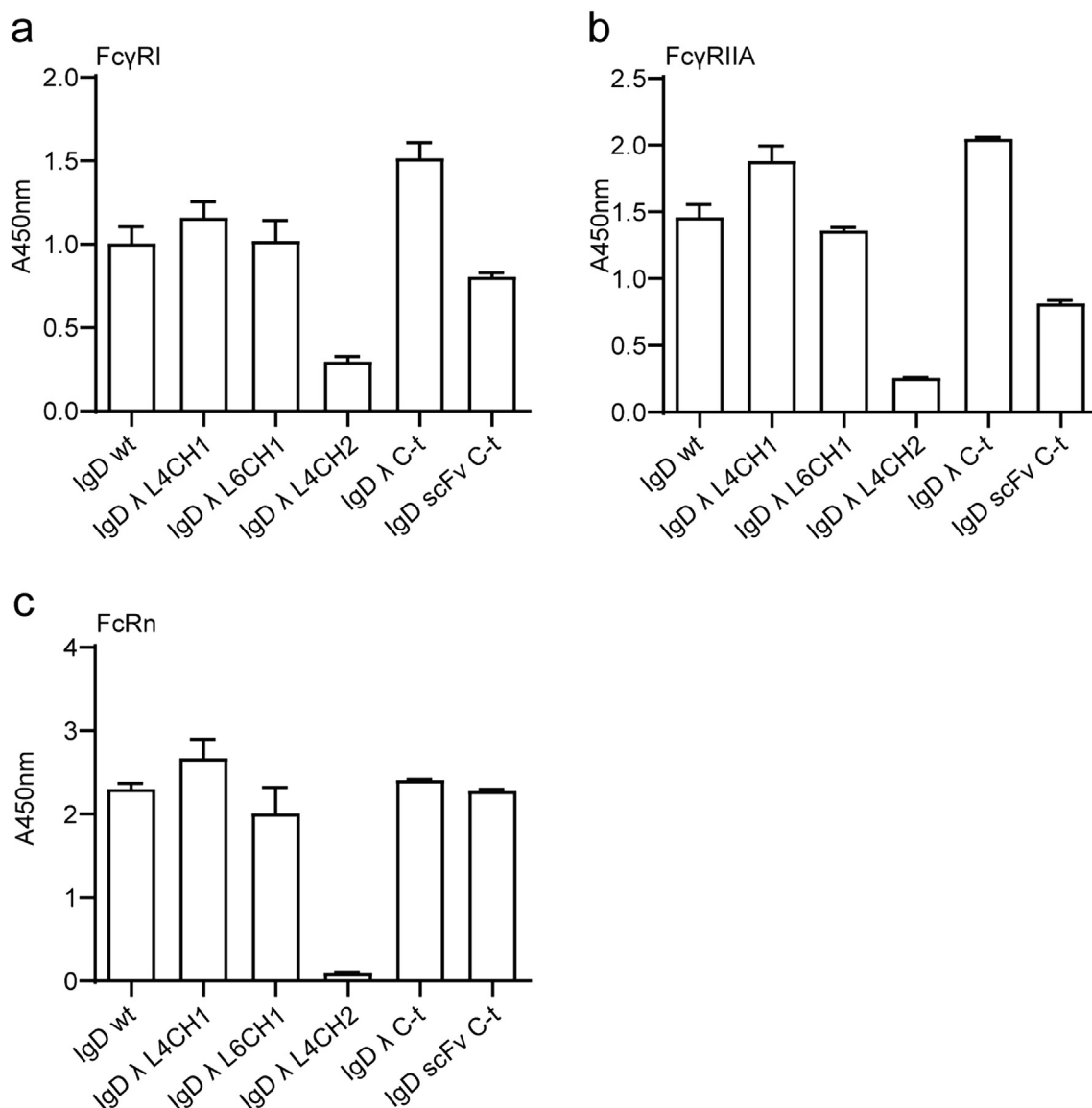


**Fig. 2.** Antibody binding to human FcRs. The ability of the antibodies to bind to a set of soluble, human FcRs was determined by ELISA. Normalized amounts of IgD-specific antibodies were added to IgD-coated plates, followed by addition of GST-tagged FcRs. Bound receptors were detected with an HRP-conjugated anti-GST mAb. Representative binding profiles for (a) Fc $\gamma$ RI, (b) Fc $\gamma$ RIIA and (c) FcRn (*n* = 2). Error bars indicate SD of mean of duplicates.

structured antibodies with heavy chain C-t fusion of either the  $\lambda$  T-cell epitope or the scFv derived from the M315 myeloma protein, which contains the  $\lambda$  T-cell epitope in its light chain variable domain (overview of the antibodies in Fig. 1a and b). To enable antigen presentation on MHC molecules, the antibodies were equipped with specificity for IgD to target B cells. The same antibodies with specificity for the hapten NIP were included as non-targeted controls.

To determine the functionality of the antibodies, we transfected HEK293E cells and assessed the structural integrity of the secreted antibodies. As determined by Western blot analysis, all antibodies were secreted as full-length hIgG antibodies of expected size (Fig. 1c). The secretion levels, however, varied (Fig. 1d). Loop exchange with  $\lambda$  as well as C-t fusion of scFv reduced the amount of secreted antibodies, to approximately 40% of wild-type (wt) for  $\lambda$  L6CH1 as well as C-t scFv, and to 15% for IgD as well as  $\lambda$  L4CH2. C-t epitope fusion positively affected the secretion level. Importantly, all antibodies bound their target IgD or NIP equally well, as assessed by ELISA (Fig. 1e).

### 3.2. Position of epitope integration affects FcR binding

FcR-mediated uptake of IgG in immune complexes is known to affect antigen presentation [27–29]. The binding site for Fc $\gamma$ Rs on

IgG is found on the upper region of CH2 and the lower hinge region, and binding depends on the presence of N-glycans attached to residue N297 in CH2 [30]. In contrast, FcRn binds IgG at the CH2-CH3 elbow region [30,31]. Therefore, we next studied if and how epitope integration affected binding of the antibodies to recombinantly expressed, soluble hFc $\gamma$ RI, hFc $\gamma$ RIIA and hFcRn in ELISA. As expected, antibodies with epitope exchange in CH1 or with C-t antigen fusion retained binding to the receptors tested (Fig. 2a-c). In contrast, the  $\lambda$  L4CH2 antibody bound neither the Fc $\gamma$ Rs nor FcRn. Loss of binding to the Fc $\gamma$ Rs was expected, as the Fc N-glycosylation site N297 is part of the native L4CH2 sequence that had been replaced by the T-cell epitope (Fig. 2a and b). The reason for lack of binding to the FcRn is not immediately clear (Fig. 2c), but the loop elongation may well infer structural changes to the CH2 domain.

### 3.3. Antibody-mediated epitope targeting induces strong T-cell activation in vitro

We next investigated the ability of the antibodies to load APCs with the  $\lambda$  epitope for presentation and activation of CD4 T cells. Irradiated splenocytes (single cell suspension generated from whole spleens) from BALB/c mice (I-E<sup>d</sup> positive) served as APCs for activation of  $\lambda$ -specific T cells, either the Th1 T-cell clone

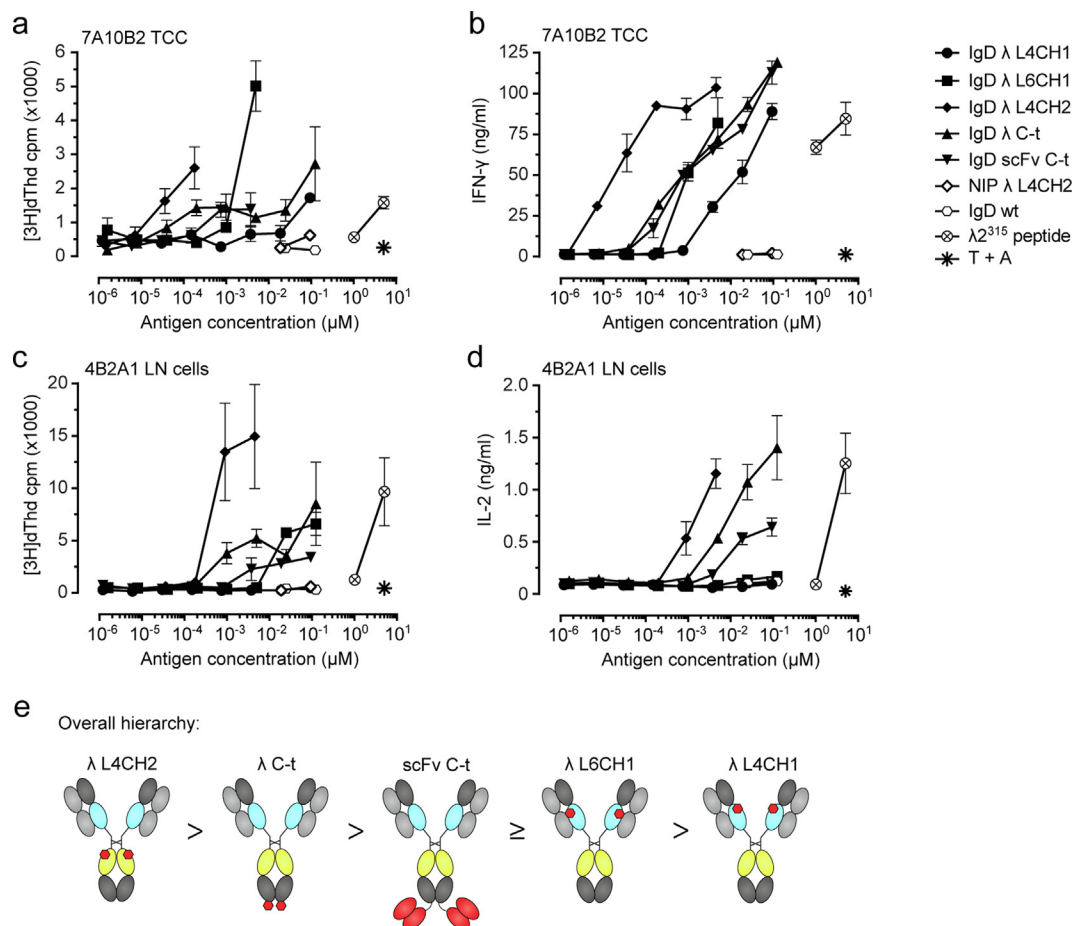


**Fig. 3.** The antibodies target APCs leading to T-cell proliferation and cytokine secretion *in vitro*. Titrated amounts of antibodies were incubated with irradiated splenocytes from BALB/c mice and T cells for 96 h before removal of supernatant for analysis of cytokine secretion, followed by addition of thymidine to the remaining cultures. (a and b) Activation of the I-E<sup>d</sup>/ $\lambda$ 2<sup>315</sup>-specific TCC 7A10B2 was measured by (a) thymidine incorporation, and (b) IFN- $\gamma$  ELISA. (c and d) T-cell activation using LN cells isolated from mice transgenic for the I-E<sup>d</sup>/ $\lambda$ 2<sup>315</sup>-specific TCR 4B2A1 as responder T cells was determined by (c) thymidine incorporation, and (d) IL-2 ELISA. (a-d) Error bars indicate SEM of triplicates; T and A represent T cells and APCs without peptide stimulation. (e) Overall hierarchy of the efficiency of the antibodies to target APCs and release the epitope based activation of 7A10B2 and 4B2A1 T cells.

(TCC) 7A10B2 or lymph node (LN) cells isolated from mice transgenic for the 4B2A1 TCR [22,23]. After *in vitro* co-culturing of APCs and T cells with titrated amounts of antibodies, we assessed T-cell activation by means of proliferation and cytokine secretion. By far, the antibody holding the T cell-epitope in L4CH2 was the most efficient vaccine construct, inducing activation of  $\lambda$ -specific T cells at 10–100-fold lower concentration than the antibodies with C-t antigen fusion, as determined by both incorporation of radioactive thymidine and cytokine secretion (Fig. 3a–d). The other antibodies also induced T-cell responses, but at much lower levels. The least effective was the IgD  $\lambda$  L4CH1 antibody, which only resulted in activation of the 7A10B2 TCC (Fig. 3a and b). Importantly, activation of  $\lambda$ -specific T cells was dependent on targeted delivery of the  $\lambda$  epitope to APCs, as the non-targeted NIP  $\lambda$  L4CH2 antibody showed responses at the same level as the IgD wt antibody without peptide (Fig. 3a–d). Furthermore, regardless of how the  $\lambda$  epitope was inte-

grated in the antibody molecules, targeting to APCs induced superior responses compared to free synthetic peptide. The overall hierarchy is summarized in Fig. 3e, with IgD  $\lambda$  L4CH2 being the most efficient antibody, followed by the C-t antigen fusions, and lastly the antibodies with the epitope in CH1.

#### 3.4. The antibodies target APCs *in vivo* after intravenous injection

To assess the ability of the antibodies to target and prime APCs *in vivo*, we injected BALB/c mice intravenously with titrated amounts of antibodies and removed spleens after 90 min. We then used the *in vivo* loaded splenocytes as APCs for *in vitro* activation of  $\lambda$ -specific T cells. We included the most potent antibody based on the previous *in vitro* assays, namely IgD  $\lambda$  L4CH2, as well as IgD  $\lambda$  L6CH1 and IgD scFv C-t. We observed strong T-cell responses which indicate that the antibodies rapidly reached the spleen, bound IgD on B cells and was endocytosed, processed and presented onto MHCII molecules. As in the previous experiments, the most efficient antibody for epitope-loading was holding the T-cell epitope in L4CH2, activating the 7A10B2 TCC to proliferate and secrete IFN- $\gamma$  at 1 log lower concentrations than IgD  $\lambda$  L6CH1 and scFv C-t (Fig. 4a and b). Additionally, only splenocytes targeted by the IgD  $\lambda$  L4CH2 antibody were able to induce IL-2 secretion from a murine BW T hybridoma expressing the  $\lambda$ -specific TCR 4B2A1 (Fig. 4c). In all experiments, intravenous injection of as little as 1  $\mu$ g IgD  $\lambda$  L4CH2 in one dose per mouse induced *in vitro* T-cell proliferation and cytokine secretion.

#### 3.5. Antibody-mediated delivery of an MHCII-restricted epitope induces memory CD8 T-cell responses *in vivo*

We next assessed if a Troycody carrying an MHCII-restricted epitope in L4CH2 would induce CD8 T-cell responses. *L. monocytogenes* is a gram-positive bacterium, causing listeriosis after consumption of contaminated food [32]. The bacteria evades host humoral responses by residing intracellularly, even infecting neighboring cells without being in contact with the extracellular milieu, and thus, the T-cell response is crucial for clearing the infection [32]. The protein Listeriolysin-O (LLO) contains an immunodominant MHCII-restricted epitope (aa 91–99 of LLO, K<sup>d</sup>-restricted) [18], and we generated antibodies carrying the LLO epitope (herein denoted LLO) in L4CH2. The antibodies were targeting CD40 which is expressed on all major APCs, including the cross-presenting DCs.

We first assessed secretion levels, and found that both CD40- and NIP-specific L4CH2 antibodies were secreted from transfected HEK293E cells, and the presence of the LLO epitope did not affect the secretion levels compared to wt (Fig. 5a). To study the *in vivo* efficacy of the LLO L4CH2 antibody to generate CD8 T-cell responses, DNA plasmids encoding antibody heavy and light chain, or NaCl alone as control, were injected into the dermis of BALB/c mice followed by electroporation. After 3 weeks the spleens were harvested and by use of IFN- $\gamma$  ELISPOT we determined LLO peptide-specific recall responses of splenocyte preparations harboring both APCs and T cells. As seen, the LLO L4CH2 antibodies induced robust IFN- $\gamma$  responses among splenocytes derived from mice immunized with the antibody-encoding plasmids, whereas the control mice which received NaCl alone did not respond to peptide stimulation (Fig. 5b). Moreover, the recall response was highly peptide-specific, because the splenocytes responded to LLO, but not to an irrelevant peptide derived from hemagglutinin (HA) or medium alone. In this assay, the non-targeted NIP LLO L4CH2 and the targeted CD40 LLO L4CH2 antibody resulted in similar, high recall responses. We speculate that this is a result of either suboptimal dosing or direct antigen presentation by electro-

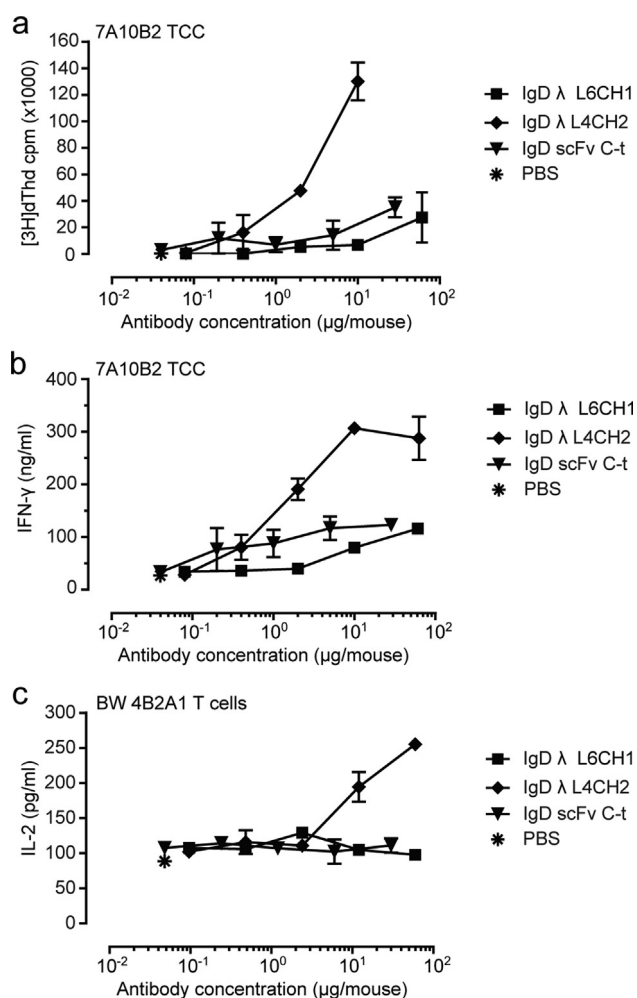


**Fig. 4.** B cells targeted *in vivo* by the IgD-specific antibodies activate T cells *in vitro*. Various concentrations of antibodies were injected intravenously into BALB/c mice (two mice per group) before mice were sacrificed after 90 min. Irradiated splenocytes were used as APCs to stimulate either 7A10B2 T cells or BW 4B2A1 hybridoma T cells. (a and b) After 72 h co-culturing of 7A10B2 T cells and APCs, supernatant samples were removed while the remaining of the cultures were pulsed with thymidine for 24 h. (a) Proliferation of the 7A10B2 T cells measured by thymidine incorporation, and (b) ELISA to determine IFN- $\gamma$  secretion levels. (c) IL-2 secretion from BW 4B2A1 hybridoma T cells was determined after 48 h of co-culturing with APCs. T-cell activation assays were performed in triplicates and the average number for each mouse was calculated. Error bars indicate SEM of the two mice.  $\lambda$  L6CH1 and L4CH2 from this experiment have been published previously [11].

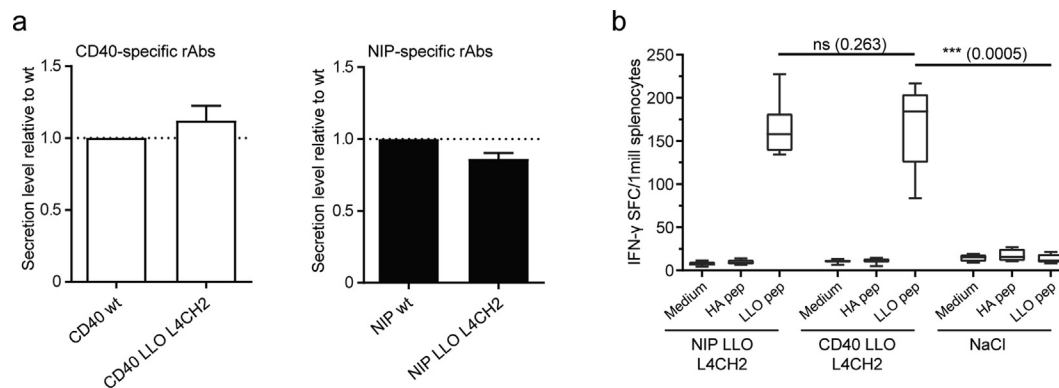


**Fig. 5.** The antibodies activate T cells *in vivo* to induce recall responses. (a) Secretion levels of CD40- and NIP-specific antibodies carrying the LLO peptide from transfected HEK293E cells was determined by ELISA after harvesting supernatants over 2 weeks. Secretion levels are shown relative to wt hlgG specific for either CD40 or NIP as indicated ( $n = 2$ ). Error bars indicate SEM of duplicates. (b) Mice were injected intradermally with antibody-encoding DNA plasmids or NaCl followed by electroporation. Spleens were harvested after 3 weeks and recall responses to the LLO peptide was assessed by IFN- $\gamma$  ELISPOT ( $n = 2$ ). Cells were stimulated with irrelevant peptide (HA = hemagglutinin) or medium alone as controls. 6 mice were immunized per group for the antibodies and 4 mice with NaCl; data is represented as boxes with the middle line at the mean and whiskers illustrating minimum and maximum values; two-tailed p-values are shown (unpaired *t*-test with Welch's correlation); \*,  $P \leq 0.05$ ; \*\*,  $P \leq 0.01$ ; \*\*\*,  $P \leq 0.001$ ; \*\*\*\*,  $P \leq 0.0001$ ; ns, not significant ( $P > 0.05$ ).

porated cells, possibly in combination with an inflammatory environment triggered by DNA injection and electroporation [33–35].

#### 4. Discussion

In this study, we have compared two modes of antibody-antigen fusion with regards to T-cell activation efficiency; antibodies carrying a T-cell epitope in Ig constant domain loops (Troybodies) and antibodies with T-cell epitope or whole antigen fused to the Ig C-t end. Although both strategies have been studied previously, this study compares the two strategies using the same system enabling a head-to-head comparison.

As found in our study, and in concordance with a previous study comparing antibodies carrying the  $\lambda$  epitope in either of the 18 loops of CH1, CH2 and CH3, the position of the inserted epitope largely impacts secretion and T-cell activation efficiency [11]. Several previous studies have utilized L6CH1 for epitope exchange and shown this loop to be extremely flexible, holding both a 37 aa long fragment containing an epitope as well as a 33 aa long gluten epitope with a complex type II polyproline helical conformation [13–15]. However, L4CH2 Troybodies are far more potent, and our data show that the L4CH2 loop, only 4 aa long, can be similarly flexible holding both a 17 aa fragment containing the  $\lambda$  epitope or the 9 aa minimal LLO epitope [11]. The efficiency of CH2 Troybodies to induce T-cell activation may be explained by the lower thermodynamic stability of CH2 compared to CH1 and CH3 [11,36–39]. Along these lines, epitope integration may further destabilize the antibody structure, translating into lower secretion levels, but also more efficient processing and epitope release.

The ability of IgG antibodies to engage effector molecules is important for modulation of the immune response. As such, binding to FcRn modulates IgG half-life, whereas binding to activating or inhibitory Fc $\gamma$ Rs aid in increasing or limiting immune responses [27–29,40,41]. Human IgG3, the IgG subclass used in this study, activates complement and Fc $\gamma$ R-mediated effector functions more efficiently than the other IgG subclasses [42]. As the N297 glycosylation site of IgG is part of L4CH2, the IgG-Fc $\gamma$ R interaction is abrogated in the L4CH2 Troybody. Accordingly, this antibody bound neither of two classical Fc $\gamma$ Rs tested, while the antibodies with C-t antigen fusion or epitope grafted into CH1 did. It was more of a surprise that the L4CH2 Troybody did not show binding to FcRn. Structurally, the L4CH2 loop is situated quite far away from the FcRn binding site at the CH2–CH3 elbow region [30,31,43]. However, the  $\beta$ -strand exiting L4CH2 enters

directly into the elbow region and contains several residues that have been shown to influence the binding of hlgG1 to FcRn [30,31]. Among these are T307, L309 and H310 (Eu numbering [44]) that are shared between hlgG1 and hlgG3. Thus, loop replacement seems to affect the CH2 structure, possibly affecting the positioning of these residues involved in the FcRn interaction. Long half-life is usually not important for a Troybody, as the vaccine molecules will be sequestered rapidly after administration or production. However, for targeting low-abundance cell types, further modulation of the Fc region to regain FcRn binding may be desired. Troybodies are monomeric and not part of immune complexes, and thus should not crosslink Fc $\gamma$ Rs. For many immunotherapeutic purposes, such as antibody-mediated clearance of malignant cells, it may be desirable to trigger complement-dependent cytotoxicity and antibody-dependent cell-mediated cytotoxicity. For targeted delivery of antigen to APCs, however, antibody binding should trigger internalization for epitope presentation, and APC killing via complement-dependent cytotoxicity or antibody-dependent cell-mediated cytotoxicity is not wanted. Furthermore, B-cell inhibition by crosslinking of B-cell receptor (BCR) and Fc $\gamma$ RIIB is equally undesirable. As such, the lack of Fc $\gamma$ R binding of the L4CH2 Troybody eliminates the need for additional Fc engineering to prevent receptor binding.

In this study, we used hlgG3 as scaffold, and there may be an anti-hlgG3 response in immunized mice. However, due to the short *in vivo* half-life of hlgG3 [45] in combination with very rapid Troybody uptake, we do not expect this to be important for the outcome.

The choice of APC cell-surface molecule targeted by antibody-antigen fusions may also affect antigen presentation levels. The cytoplasmic tails of surface molecules such as IgD and CD40 contain intracellular motifs that allow for internalization, signaling and directional intracellular sorting. Late endosomal compartments are associated with MHCII presentation and contain accessory molecules involved in the MHCII pathway such as HLA-DM and proteases, whereas early endosomal compartments are associated with cross-presentation on MHCI [1,46,47]. Ligation of the BCR on the B-cell surface triggers internalization of the BCR and its bound cargo, and at the same time, induces maturation of antigen-processing compartments in which both the antigen, MHCII and accessory molecules converge [48]. As such, the BCR is a suitable molecule to target for MHCII presentation and engagement of B cells. In contrast to intracellular sorting of the BCR, CD40



is routed to early endosomal compartments involved in cross-presentation [49]. We have previously shown that the rat IgG2a antibody (clone FGK45) from which the CD40-specific mouse V genes were cloned functions in an agonistic fashion by inducing proliferation of splenocytes, secretion of IL-12p40 from DCs and upregulation of CD54, CD86 and MHCII by DCs [15]. Others have demonstrated that ligation of CD40 by agonistic anti-CD40 antibodies can bypass the need for CD4 T cells in the licensing of CD8 T cells [50]. This is a prerequisite when targeting a CD8 T-cell epitope only. Additionally, a plethora of other APC targets have been explored, including antibody-mediated targeting of antigen to DEC-205 (CD205), the mannose receptor (CD206), DC-SIGN (CD209) and CD11c [51–54]. Besides targeting by use of specific antibodies, antigen have also been fused to chemokines for targeting of chemokine receptor expressed on APCs, such as the CCL3:CCR1/CCR3 and XCL1/XCR1 ligand:receptor pairs [55–59].

Here we describe design of Trojans that induce T-cell responses against a myeloma protein and an infectious disease, respectively. An interesting use of antibodies such as those we describe, is in cancer immunotherapy in combination with checkpoint inhibitors. As the breaks on T cells are lifted by use of anti-PD1, anti-CTLA4 or other approaches, efficient targeting of antigenic peptides to APCs could aid in boosting the activation of antigen-specific T cells.

#### Declaration of Competing Interest

The authors declare that they have no known competing financial interests or personal relationships that could have appeared to influence the work reported in this paper.

#### Acknowledgements

This work was supported by the Research Council of Norway through its Centers of Excellence funding scheme, under project number 179573/V40. We are grateful to Sivaganesh Sathiaruby for technical assistance.

#### References

- Rock KL, Reits E, Neefjes J. Present Yourself! By MHC Class I and MHC Class II Molecules. *Trends Immunol* 2016;37(11):724–37.
- Bevan MJ. Cross-priming for a secondary cytotoxic response to minor H antigens with H-2 congenic cells which do not cross-react in the cytotoxic assay. *J Exp Med* 1976;143(5):1283–8.
- Bevan MJ. Minor H antigens introduced on H-2 different stimulating cells cross-react at the cytotoxic T cell level during in vivo priming. *J Immunol* 1976;117(6):2233–8.
- Moyle PM, Toth I. Modern subunit vaccines: development, components, and research opportunities. *ChemMedChem* 2013;8(3):360–76.
- Hos BJ et al. Approaches to Improve Chemically Defined Synthetic Peptide Vaccines. *Front Immunol* 2018;9:884.
- Lunde E et al. Antibodies engineered with IgD specificity efficiently deliver integrated T-cell epitopes for antigen presentation by B cells. *Nat Biotechnol* 1999;17(7):670–5.
- Baier G et al. Immunogenic targeting of recombinant peptide vaccines to human antigen-presenting cells by chimeric anti-HLA-DR and anti-surface immunoglobulin D antibody Fab fragments in vitro. *J Virol* 1995;69(4):2357–65.
- Bonifaz L et al. Efficient targeting of protein antigen to the dendritic cell receptor DEC-205 in the steady state leads to antigen presentation on major histocompatibility complex class I products and peripheral CD8+ T cell tolerance. *J Exp Med* 2002;196(12):1627–38.
- Hawiger D et al. Dendritic cells induce peripheral T cell unresponsiveness under steady state conditions in vivo. *J Exp Med* 2001;194(6):769–79.
- Lunde E, Bogen B, Sandlie I. Immunoglobulin as a vehicle for foreign antigenic peptides immunogenic to T cells. *Mol Immunol* 1997;34(16–17):1167–76.
- Flobakk M et al. Processing of an antigenic sequence from IgG constant domains for presentation by MHC class II. *J Immunol* 2008;181(10):7062–72.
- Rasmussen IB et al. CD40/APC-specific antibodies with three T-cell epitopes loaded in the constant domains induce CD4+ T-cell responses. *Protein Eng Des Sel* 2012;25(3):89–96.
- Tunheim G et al. Recombinant antibodies for delivery of antigen: a single loop between beta-strands in the constant region can accommodate long, complex and tandem T cell epitopes. *Int Immunol* 2008;20(3):295–306.
- Lunde E et al. Efficient delivery of T cell epitopes to APC by use of MHC class II-specific Trojans. *J Immunol* 2002;168(5):2154–62.
- Schjetne KW, Fredriksen AB, Bogen B. Delivery of antigen to CD40 induces protective immune responses against tumors. *J Immunol* 2007;178(7):4169–76.
- Eisen HN, Simms ES, Potter M. Mouse myeloma proteins with antihapten antibody activity. The protein produced by plasma cell tumor MOPC-315. *Biochemistry* 1968;7(11):4126–34.
- Bogen B, Lambris JD. Minimum length of an idiotype peptide and a model for its binding to a major histocompatibility complex class II molecule. *EMBO J* 1989;8(7):1947–52.
- Harty JT, Bevan MJ. CD8+ T cells specific for a single nonamer epitope of *Listeria monocytogenes* are protective in vivo. *J Exp Med* 1992;175(6):1531–8.
- Norderhaug L et al. Versatile vectors for transient and stable expression of recombinant antibody molecules in mammalian cells. *J Immunol Methods* 1997;204(1):77–87.
- Neuberger MS. Expression and regulation of immunoglobulin heavy chain gene transferred into lymphoid cells. *EMBO J* 1983;2(8):1373–8.
- Horton RM et al. Gene splicing by overlap extension: tailor-made genes using the polymerase chain reaction. *Biotechniques* 1990;8(5):528–35.
- Bogen B et al. Weak positive selection of transgenic T cell receptor-bearing thymocytes: importance of major histocompatibility complex class II, T cell receptor and CD4 surface molecule densities. *Eur J Immunol* 1992;22(3):703–9.
- Bogen B, Malissen B, Haas W. Idiotope-specific T cell clones that recognize syngeneic immunoglobulin fragments in the context of class II molecules. *Eur J Immunol* 1986;16(11):1373–8.
- Berntzen G et al. Prolonged and increased expression of soluble Fc receptors, IgG and a TCR-Ig fusion protein by transiently transfected adherent 293E cells. *J Immunol Methods* 2005;298(1–2):93–104.
- Andersen JT et al. Ligand binding and antigenic properties of a human neonatal Fc receptor with mutation of two unpaired cysteine residues. *FEBS J* 2008;275(16):4097–110.
- Roos AK et al. Enhancement of cellular immune response to a prostate cancer DNA vaccine by intradermal electroporation. *Mol Ther* 2006;13(2):320–7.
- Qiao SW et al. Dependence of antibody-mediated presentation of antigen on FcRn. *Proc Natl Acad Sci USA* 2008;105(27):9337–42.
- Mi W et al. Targeting the neonatal Fc receptor for antigen delivery using engineered Fc fragments. *J Immunol* 2008;181(11):7550–61.
- Guilliams M et al. The function of Fcγ receptors in dendritic cells and macrophages. *Nat Rev Immunol* 2014;14(2):94–108.
- Shields RL et al. High resolution mapping of the binding site on human IgG1 for FcγRI, FcγRII, FcγRIII, and FcRn and design of IgG1 variants with improved binding to the FcγRI. *J Biol Chem* 2001;276(9):6591–604.
- Kim JK et al. Mapping the site on human IgG for binding of the MHC class I-related receptor, FcRn. *Eur J Immunol* 1999;29(9):2819–25.
- Radoshevich L, Cossart P. *Listeria monocytogenes*: towards a complete picture of its physiology and pathogenesis. *Nat Rev Microbiol* 2018;16(1):32–46.
- Todorova B et al. Electroporation as a vaccine delivery system and a natural adjuvant to intradermal administration of plasmid DNA in macaques. *Sci Rep* 2017;7(1):4122.
- Roos AK et al. Skin electroporation: effects on transgene expression, DNA persistence and local tissue environment. *PLoS ONE* 2009;4(9):e7226.
- Andersen TK et al. Enhanced germinal center reaction by targeting vaccine antigen to major histocompatibility complex class II molecules. *npj Vaccines* 2019;4:9.
- Feige MJ, Walter S, Buchner J. Folding mechanism of the CH2 antibody domain. *J Mol Biol* 2004;344(1):107–18.
- Rothlisberger D, Honegger A, Pluckthun A. Domain interactions in the Fab fragment: a comparative evaluation of the single-chain Fv and Fab format engineered with variable domains of different stability. *J Mol Biol* 2005;347(4):773–89.
- Lesk AM, Chothia C. Elbow motion in the immunoglobulins involves a molecular ball-and-socket joint. *Nature* 1988;335(6186):188–90.
- Dall'Acqua W et al. Contribution of domain interface residues to the stability of antibody CH3 domain homodimers. *Biochemistry* 1998;37(26):9266–73.
- Ward ES et al. Evidence to support the cellular mechanism involved in serum IgG homeostasis in humans. *Int Immunol* 2003;15(2):187–95.
- Roopenian DC et al. The MHC class I-like IgG receptor controls perinatal IgG transport, IgG homeostasis, and fate of IgG-Fc-coupled drugs. *J Immunol* 2003;170(7):3528–33.
- Dekkers G et al. Affinity of human IgG subclasses to mouse Fcγ receptors. *MAbs* 2017;9(5):767–73.
- Andersen JT et al. Anti-carcinoma embryonic antigen single-chain variable fragment antibody variants bind mouse and human neonatal Fc receptor with different affinities that reveal distinct cross-species differences in serum half-life. *J Biol Chem* 2012;287(27):22927–37.
- Edelman GM et al. The covalent structure of an entire gammaG immunoglobulin molecule. *Proc Natl Acad Sci USA* 1969;63(1):78–85.
- Stapleton NM et al. Competition for FcRn-mediated transport gives rise to short half-life of human IgG3 and offers therapeutic potential. *Nat Commun* 2011;2:599.

- [46] Burgdorf S et al. Distinct pathways of antigen uptake and intracellular routing in CD4 and CD8 T cell activation. *Science* 2007;316(5824):612–6.
- [47] Cruz FM et al. The Biology and Underlying Mechanisms of Cross-Presentation of Exogenous Antigens on MHC-I Molecules. *Annu Rev Immunol* 2017;35:149–76.
- [48] Adler LN et al. The Other Function: Class II-Restricted Antigen Presentation by B Cells. *Front Immunol* 2017;8:319.
- [49] Chatterjee B et al. Internalization and endosomal degradation of receptor-bound antigens regulate the efficiency of cross presentation by human dendritic cells. *Blood* 2012;120(10):2011–20.
- [50] Schuurhuis DH et al. Immature dendritic cells acquire CD8(+) cytotoxic T lymphocyte priming capacity upon activation by T helper cell-independent or -dependent stimuli. *J Exp Med* 2000;192(1):145–50.
- [51] Mahnke K et al. The dendritic cell receptor for endocytosis, DEC-205, can recycle and enhance antigen presentation via major histocompatibility complex class II-positive lysosomal compartments. *J Cell Biol* 2000;151(3):673–84.
- [52] Guermonprez P et al. In vivo receptor-mediated delivery of a recombinant invasive bacterial toxoid to CD11c + CD8 alpha -CD11bhigh dendritic cells. *Eur J Immunol* 2002;32(11):3071–81.
- [53] Trumpfheller C et al. Intensified and protective CD4+ T cell immunity in mice with anti-dendritic cell HIV gag fusion antibody vaccine. *J Exp Med* 2006;203(3):607–17.
- [54] Schjetne KW et al. A mouse C kappa-specific T cell clone indicates that DC-SIGN is an efficient target for antibody-mediated delivery of T cell epitopes for MHC class II presentation. *Int Immunol* 2002;14(12):1423–30.
- [55] Ruffini PA et al. Human chemokine MIP1alpha increases efficiency of targeted DNA fusion vaccines. *Vaccine* 2010;29(2):191–9.
- [56] Fossum E et al. Vaccine molecules targeting Xcr1 on cross-presenting DCs induce protective CD8+ T-cell responses against influenza virus. *Eur J Immunol* 2015;45(2):624–35.
- [57] Øynebraten I et al. Increased generation of HIV-1 gp120-reactive CD8+ T cells by a DNA vaccine construct encoding the chemokine CCL3. *PLoS ONE* 2014;9(8):e104814.
- [58] Biragyn A et al. Genetic fusion of chemokines to a self tumor antigen induces protective, T-cell dependent antitumor immunity. *Nat Biotechnol* 1999;17(3):253–8.
- [59] Biragyn A et al. Mediators of innate immunity that target immature, but not mature, dendritic cells induce antitumor immunity when genetically fused with nonimmunogenic tumor antigens. *J Immunol* 2001;167(11):6644–53.
- [60] Saphire EO et al. Crystal structure of a neutralizing human IGG against HIV-1: a template for vaccine design. *Science* 2001;293(5532):1155–9.